

Substitution Effects of In^{3+} by Al^{3+} and Ga^{3+} on the Photocatalytic and Structural Properties of the $\text{Bi}_2\text{InNbO}_7$ Photocatalyst

Zhigang Zou,^{*,†} Jinhua Ye,[‡] and Hironori Arakawa[†]

National Institute of Materials and Chemical Research, 1–1 Higashi, Tsukuba, Ibaraki 305, Japan, and National Research Institute for Metals, 1-2-1 Sengen, Tsukuba, Ibaraki 305, Japan

Received August 24, 2000. Revised Manuscript Received February 21, 2001

A new series of photocatalysts, Bi_2MNbO_7 ($\text{M} = \text{Al}^{3+}, \text{Ga}^{3+}, \text{In}^{3+}$), were synthesized by solid-state reaction and characterized by powder X-ray diffraction and Rietveld structure refinement. The substitution effect of In^{3+} by Al^{3+} and Ga^{3+} on the photocatalytic and structural properties of the $\text{Bi}_2\text{InNbO}_7$ photocatalyst was investigated. These photocatalysts crystallize in the same pyrochlore structure, but the lattice parameters decrease with decreasing M^{3+} ($\text{M}^{3+} = \text{Al}^{3+}, \text{Ga}^{3+}, \text{In}^{3+}$) ionic radii. The rates of H_2 and O_2 evolution from an aqueous methanol and cerium sulfate solution significantly increases with decreasing M^{3+} ionic radii under UV irradiation. The $\text{Bi}_2\text{AlNbO}_7$ photocatalyst exhibits much higher photocatalytic activity than the well-known TiO_2 photocatalyst.

Introduction

The processes of photocatalytic decomposition of water with the TiO_2 photocatalyst were extensively studied during the past decade.^{1–4} Photocatalysis processes involve the initial absorption of photons by band gap of TiO_2 and generating electron/hole pairs in the TiO_2 surface. However, the efficiency of the photoinduced chemistry is limited by the light absorption characteristics of TiO_2 . The search for new materials with higher activity than that of TiO_2 has been one of the most active areas in heterogeneous photocatalysis.^{5–7} However, until now the number of photocatalysts has been limited.

Very recently, we reported a new photocatalyst, the $\text{Bi}_2\text{InNbO}_7$ semiconductor.⁸ The semiconductor has a band gap of ~ 2.7 eV and seems to have potential to improve the activity by modifying the electron and crystal structures of the photocatalyst.⁸ $\text{Bi}_2\text{InNbO}_7$ belongs to the family of the $\text{A}_2\text{B}_2\text{O}_7$ compounds with the $\text{A}^{3+}_2\text{B}^{4+}_2\text{O}_7$ pyrochlore structure. We considered that M^{3+} ($\text{M}^{3+} = \text{Al}^{3+}, \text{Ga}^{3+}, \text{In}^{3+}$) and Nb^{5+} substitution of the B^{4+} sites in $\text{A}^{3+}_2\text{B}^{4+}_2\text{O}_7$ might cause an increase in hole(carrier) concentration and provide a change in

photocatalytic and photophysical properties. In addition, a change of M^{3+} ionic radii in the B^{4+} site might cause a slight modification of crystal structure, resulting in delocalization of the charge carriers. The improvement in mobility of the charge is important for photocatalysts. The mobility of charge affects the photocatalytic activity because it affects the probability of electrons reaching reaction sites on the surface of the photocatalyst. A slight modification of the structure of the semiconductor has a dramatic effect on the charge mobility.⁹ However, the effects of modification of the structure by controlling the ionic radius of photocatalysts in order to improve the activity of the photolysis of water have not been reported. Here we report the synthesis, photocatalytic, and structural characterizations of the Bi_2MNbO_7 ($\text{M} = \text{Al}^{3+}, \text{Ga}^{3+}, \text{In}^{3+}$) photocatalysts. A comparison of the photocatalytic properties of Bi_2MNbO_7 to that of the TiO_2 photocatalyst is presented.

Experimental Section

The polycrystalline samples of the Bi_2MNbO_7 ($\text{M} = \text{Al}^{3+}, \text{Ga}^{3+}, \text{In}^{3+}$) photocatalysts were prepared by solid-state reaction with high purity grade chemicals of $\text{Bi}_2(\text{CO}_3)_3$, In_2O_3 , Nb_2O_5 , $\alpha\text{-Al}_2\text{O}_3$, and Ga_2O_3 . The stoichiometric amounts of precursors were mixed and pressed into small pellets. The pellets were reacted on an aluminum crucible in air three times. In the final process, the column samples were reacted for 2 days at 1100 °C.

The chemical composition of the samples before and after the photocatalytic reactions was determined by a scanning electron microscope X-ray energy dispersion spectrum (SEM-EDS) with an accelerating voltage of 25 kV. The powder X-ray diffraction (PDX) pattern of the Bi_2MNbO_7 photocatalysts was measured with $\text{Cu K}\alpha$ radiation ($\lambda = 1.54178$ Å). The UV–vis diffuse reflectance spectrum of Bi_2MNbO_7 was measured by

* To whom correspondence should be addressed. Tel: +81-298-61-4750. Fax: +81-298-61-4750. E-mail: zou@nimc.go.jp

[†] National Institute of Materials and Chemical Research.

[‡] National Research Institute for Metals.

(1) Honda, K.; Fujishima, A. *Nature* **1972**, *238*, 37.

(2) Kawai, T.; Sakata, T. *Nature* **1980**, *286*, 474.

(3) Geoffrey, B. S.; Thomas, E. M. *J. Phys. Chem. B* **1997**, *101*, 2508.

(4) Yeong, K.; Samer, S.; Munir, J. H.; Thomas, E. M. *J. Am. Chem. Soc.* **1991**, *113*, 9561.

(5) Sayama, K.; Yase, K.; Arakawa, H.; Asakura, K.; Tanaka, K.; Domen, K.; Onishi, T. *J. Photochem. Photobiol. A* **1998**, *114*, 125.

(6) Takata, T.; Tanaka, A.; Hara, M.; Kodo, J.; Domen, K. *Catal. Today* **1998**, *44*, 17.

(7) Kakuta, N.; Gota, N.; Ohkita, H.; Mizushima, T. *J. Phys. Chem. B* **1999**, *103*, 5917.

(8) Zou, Z.; Ye, J.; Arakawa, H. *J. Mater. Sci. Lett.* **2000**, *19*, 1909.

Zou, Z.; Ye, J.; Abe, R.; Arakawa, H. *Catal. Lett.* **2000**, *68*, 235.

(9) Zou, Z.; Ye, J.; Oka, K.; Nishihara, Y. *Phys. Rev. Lett.* **1998**, *80*, 1074.

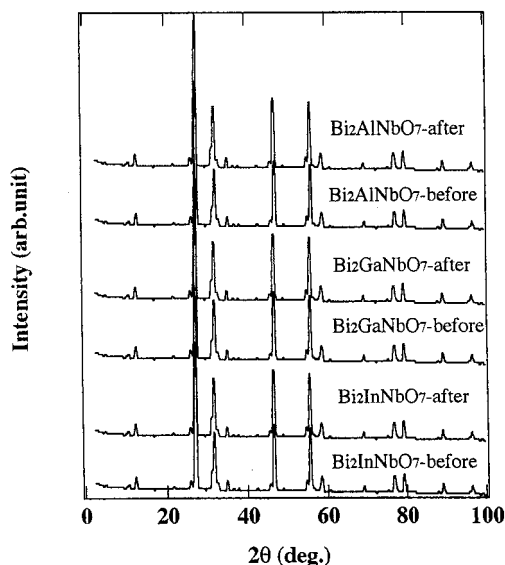


Figure 1. A comparison of XRD patterns of Bi_2MNbO_7 ($M = \text{Al}^{3+}, \text{Ga}^{3+}, \text{In}^{3+}$) before and after photocatalytic reactions.

with a UV-vis spectrometer (MPS-2000). The surface area was determined by BET measurement (Micromeritics, Shimadzu, FlowPrep 060).

The photocatalytic reaction was examined using a gas-closed circulation system and an inner-irradiation type quartz cell with a 400 W high-pressure Hg lamp. The gases evolved were determined with a TCD gas chromatograph, which was connected with a circulating line.⁸ To obtain high activity, it is essential to load a metal or metal oxide on the surface of the photocatalyst. The Pt was found to be the most effective for the TiO_2 photocatalyst, since Pt can change the surface properties of the TiO_2 photocatalyst and, hence, its photocatalytic behavior.¹⁰ The photocatalytic reaction was performed in an aqueous $\text{CH}_3\text{OH}/\text{H}_2\text{O}$ solution (1.0 g powder catalyst, 50 mL CH_3OH , 350 mL H_2O , and 0.1 wt % Pt (Pt-loading instead of a H_2PtCl_4)).⁸ O_2 evolution was performed in an aqueous cerium sulfate tetrahydrate solution (1.0 g powder catalyst, 1.0 m mol $\text{Ce}(\text{SO}_4)_2$, 400 mL H_2O), since that solution is more stable than an aqueous silver nitrate under UV irradiation.¹¹

Results and Discussion

Powder X-ray diffraction data of Bi_2MNbO_7 ($M = \text{Al}^{3+}, \text{Ga}^{3+}, \text{In}^{3+}$) were collected with a step scan procedure in the range of $2\theta = 5\text{--}100^\circ$. The step interval was 0.024° and scan speed was 1°min^{-1} . In Figure 1, the PXD patterns of the Bi_2MNbO_7 photocatalysts show that Bi_2MNbO_7 ($M = \text{Al}^{3+}, \text{Ga}^{3+}, \text{In}^{3+}$) are the single phases. This is consistent with the observation from SEM-EDS. Although the Bi_2MNbO_7 photocatalysts showed similar PXD patterns, the 2θ angles of reflections shifted with variation of M ($M = \text{Al}^{3+}, \text{Ga}^{3+}, \text{In}^{3+}$). The 2θ angle change in the PXD patterns suggests that the lattice parameter changes with In^{3+} being substituted by Al^{3+} and Ga^{3+} . Full-profile structure refinement of the collected powder diffraction data was performed with the Rietveld program RIETAN.¹² Positional parameters and isotropic thermal parameters of Bi_2MNbO_7 ($M = \text{Al}^{3+}, \text{Ga}^{3+}, \text{In}^{3+}$) were refined. The starting parameters of the refinement were based on the pyrochlore structure, that is, which pyrochlore

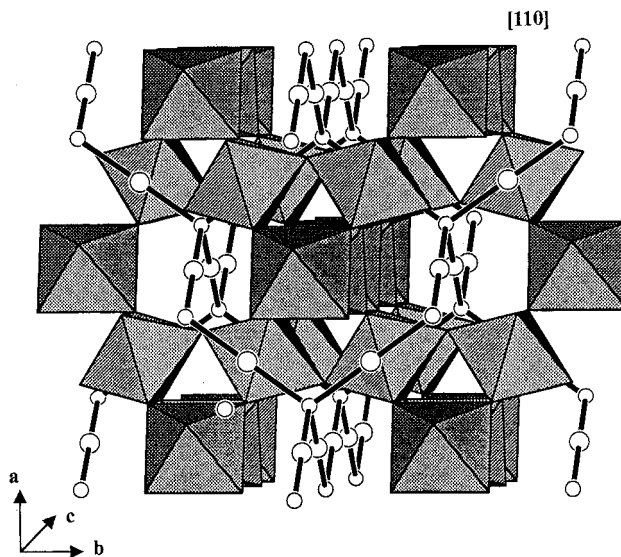


Figure 2. The schematic structural diagram of Bi_2MNbO_7 ($M^{3+} = \text{Al}^{3+}, \text{Ga}^{3+}, \text{In}^{3+}$). Three-dimensional network of MO_6 stacked along $[001]$ and separated by a unit cell translation.

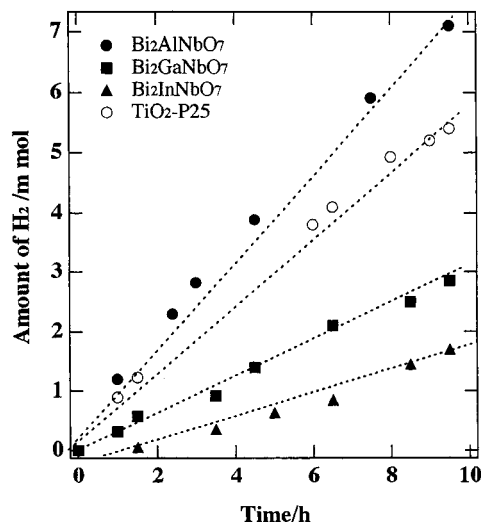


Figure 3. Photocatalytic H_2 evolutions on Bi_2MNbO_7 ($M = \text{Al}^{3+}, \text{Ga}^{3+}, \text{In}^{3+}$) and $\text{TiO}_2(\text{P-25})$ from $\text{CH}_3\text{OH}/\text{H}_2\text{O}$ solution under UV irradiation. Cat., 1.0 g; CH_3OH , 50 mL; H_2O , 350 mL; 400 W high-pressure Hg lamp.

structure was used for initial Rietveld refinement. The detailed investigations on the structure indicated that they form a three-dimensional corner-sharing octahedral MO_6 ($M = \text{Al}^{3+}, \text{Ga}^{3+}, \text{In}^{3+}$ and Nb^{5+}) in the network structure of Bi_2MNbO_7 . Figure 2 shows the schematic diagram of the pyrochlore type structure of Bi_2MNbO_7 ($M^{3+} = \text{Al}^{3+}, \text{Ga}^{3+}, \text{In}^{3+}$). The MO_6 ($M = \text{Al}^{3+}, \text{Ga}^{3+}, \text{In}^{3+}$ and Nb^{5+}) are connected into chains with the Bi ions. Although the Bi_2MNbO_7 ($M^{3+} = \text{Al}^{3+}, \text{Ga}^{3+}, \text{In}^{3+}$) photocatalysts crystallize in the same pyrochlore-type crystal structure, (cubic, space group $Fd\bar{3}m$), the lattice parameters decrease with the decreasing effective ionic radius of M^{3+} ($M^{3+} = \text{Al}^{3+}, \text{Ga}^{3+}, \text{In}^{3+}$), $\text{Al}^{3+} < \text{Ga}^{3+} < \text{In}^{3+}$ (see Table 1). All the diffraction peaks for the Bi_2MNbO_7 photocatalysts could be successfully indexed based on the lattice parameters and the space group.

The photocatalysts were suspended in the $\text{CH}_3\text{OH}/\text{H}_2\text{O}$ and $\text{Ce}(\text{SO}_4)_2/\text{H}_2\text{O}$ solutions, respectively. H_2 evolution was generated from the $\text{CH}_3\text{OH}/\text{H}_2\text{O}$ solution under UV irradiation and the results are shown in Figure 3.

(10) Kim, H. G.; Hwang, D. W.; Kim, J.; Kim, Y. G.; Lee, J. *Chem. Commun.* **1999**, 1077.

(11) Meulenkamp, E. A.; Wrr, A. R. *Electrochim. Acta* **1996**, *41*, 109.

(12) Izumi, F. *J. Crystallogr. Assoc. Jpn.* **1985**, *27*, 23.

Table 1. Rates of Gas Evolution and Physical Properties of the Photocatalysts

photocatalyst	type of structure	lattice parameter <i>a</i> (Å)	surface area m ² /g	rate of gas evolutions (μ mol h ⁻¹) ^a		
				CH ₃ OH/H ₂ O ^b		Ce(SO ₄) ₂ /H ₂ O
				H ₂	CO	O ₂
Bi ₂ AlNbO ₇	pyrochlore	10.7171(2)	0.51	710	32	25
Bi ₂ GaNbO ₇	pyrochlore	10.7342(2)	0.52	300	7	10
Bi ₂ InNbO ₇	pyrochlore	10.7793(2)	0.51	180	5	7
TiO ₂ (P25) ⁵	anatase + rutile		53.80	550	15	17

^a Light source: 400 W high-pressure Hg lamp. Cat., 1.0 g. ^b 0.1 wt % Pt instead of a H₂PtCl₆ was loaded on the surface of the powder catalysts.

The formation rate of H₂ evolution increased significantly with decreasing M³⁺ ionic radii. This means that the activity of these photocatalysts increases with decreasing M³⁺ ionic radii. The formation rates of H₂ evolution was estimated to be 0.71, 0.3, and 0.18 mmol g⁻¹ h⁻¹ in the first 10 h for Al³⁺, Ga³⁺, In³⁺, respectively. The total amount of H₂/catalyst(mol) for these photocatalysts was much greater than 1.0 at 10 h, indicating that the reaction occurs catalytically. It is noted that the formation rate of H₂ evolution with Bi₂AlNbO₇ is much larger than that of the well-known TiO₂ photocatalyst (TiO₂-P25, see Table 1). This means that the activity of Bi₂AlNbO₇ is higher than that of the TiO₂ photocatalyst. The CO evolution was observed as the oxidation product in this reaction (see Table 1). However, the formation rate of CO evolution is much lower than that of H₂ evolution. The ratios of nonstationary and nonstoichiometric evolutions between H₂ and CO might result from generation of CO₂ and other gases. It is well-known that when CH₃OH is added to a Pt/TiO₂ aqueous suspension, sustained H₂ production is observed under UV irradiation and the alcohol molecules are oxidized to final products of CO₂, CO, CH₄, etc.⁸ The presence of oxygen vacancy defects strongly enhances such interaction due to electron back-donation from surface Ti³⁺ into π* orbitals of molecular CO.⁸ The CO evolution increases with illumination time as does H₂ evolution. The formation rate of CO increased with decreasing M (M = Al³⁺, Ga³⁺, In³⁺), showing the same tendency as observed in H₂ evolutions. The rate of CO evolution in Bi₂AlNbO₇ is also much larger than that in the TiO₂ photocatalyst.

The O₂ evolution reaction was performed in an aqueous cerium sulfate tetrahydrate solution and only the following stoichiometric reaction occurred: 4Ce⁴⁺ + 2H₂O → 4Ce³⁺ + O₂ + 4H⁺. The aqueous Ce(SO₄)₂ solution is more stable than aqueous silver nitrate under UV irradiation since photodeposition of Ce³⁺ did not occur after illumination.¹¹ However, the reaction, 2NO₃⁻ → 2NO₂⁻ + O₂, might occur in an aqueous AgNO₃ solution under UV irradiation since NO₃⁻ is unstable, excepting the reaction, 4Ag⁺ + 2H₂O → 4Ag⁰ + O₂ + 4H⁺.¹³ The rate of O₂ evolution in the first 10 h increased rapidly with decreasing M³⁺ ionic radii. The results are shown in Table 1. This means that the photocatalysts have potential for O₂ evolution from aqueous solution and the activity for O₂ evolution increases with decreasing M³⁺ ionic radii. The rate of O₂ and H₂ evolution for Bi₂AlNbO₇ is larger than that of the TiO₂ photocatalyst from CH₃OH/H₂O solution.

It is known that the photooxidation/photodissolution of a catalyst might consume oxygen. However, such reactions generally lead to changes of crystal structure and the chemical composition of photocatalyst. We examined the atomic ratio and the crystal structure of these photocatalysts before and after reactions. The chemical composition of the photocatalysts was determined using characteristic X-rays of Al Lα, Ga Lα, In Lα, Nb Lα, and Bi Mα. The composition content was decided using the ZAF quantification method. The SEM-EDS analysis showed that the compounds have a homogeneous atomic distribution. The crystalline grains of the samples have a maximum size of about 6.0 μm. The atomic ratio of these photocatalysts was confirmed by XRFS (X-ray fluorescence spectrometer) measurement. The observation is in agreement with results of SEM-EDS analysis. Oxygen content was calculated from the EDS results.⁹ All samples before and after the reactions have similar chemical composition according to the observation of SEM-EDS and XRFS analyses. There is no chemical reaction between the samples and the containing crucibles. There are no changes of Bi₂MNbO₇ (M = Al³⁺, Ga³⁺, In³⁺) before or after photocatalytic reactions from PXD patterns as shown in Figure 1. From these experimental results we confirmed that the photocatalysts before and after photocatalytic reactions have not changed in either crystal structure or chemical composition.

The effect of UV illumination was also investigated. Figure 4 shows the results for response to UV illumination for Bi₂AlNbO₇. The reaction stopped when the light was turned off, showing the obvious light response. This result shows that the photocatalytic reaction is induced by the absorption of UV irradiation. The reaction was stopped after 30 h for the first time, and the reacted solution was deflated again, then re-reacted. The activity did not exhibit obvious decrease with reaction time. This suggests that the photocatalytic activity of Bi₂AlNbO₇ is stable under UV irradiation.

We investigated the light absorption properties of Bi₂MNbO₇ (M = Al³⁺, Ga³⁺, In³⁺) photocatalysts. Figure 5 shows the result of diffuse reflection spectra. The onset of diffuse reflection spectra of these photocatalysts showed an obvious shift to lower wavelength with decreasing M³⁺ ionic radii. The band gaps of the Bi₂MNbO₇ photocatalysts were estimated to be about 2.9, 2.75, and 2.7 eV, respectively, from the onset of diffuse reflection spectra (Figure 5). Thus, the band gaps of these photocatalysts increase with decreasing M³⁺ ionic radii. The band structure of oxides is generally defined by *d*-level and O *2p*-level. Scaife examined that the valence band energy should be assumed by the O

(13) Tada, H.; Hattori, A.; Tokihisa, Y.; Imai, K.; Tohee, N.; Ito, S. *J. Phys. Chem. B* **2000**, *104*, 4585.

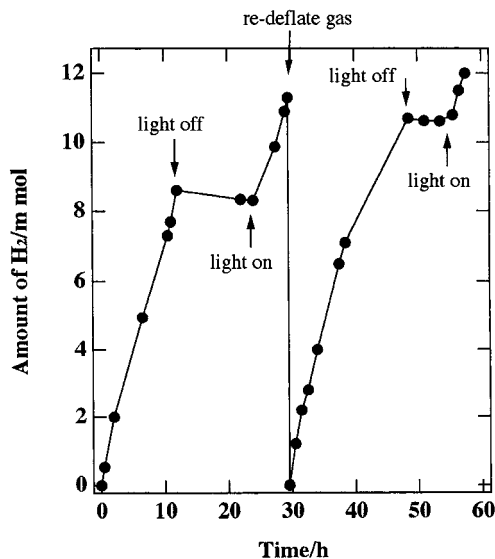


Figure 4. Response of UV light and reappearing reaction for $\text{Bi}_2\text{AlNbO}_7$ in $\text{CH}_3\text{OH}/\text{H}_2\text{O}$ solution. Cat., 1.0 g; CH_3OH , 50 mL; H_2O , 350 mL; 400 W high-pressure Hg lamp.

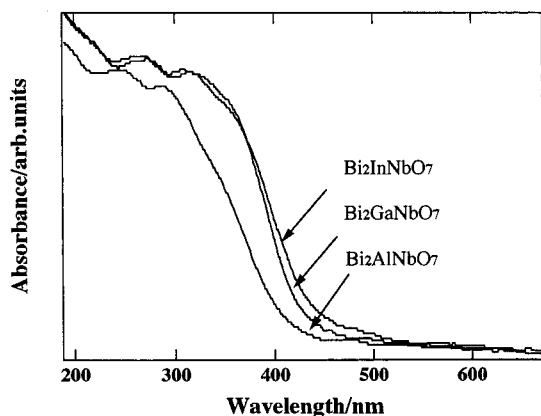


Figure 5. Diffuse reflectance spectrums of $\text{Bi}_2\text{MnNbO}_7$ ($M = \text{Al}^{3+}, \text{Ga}^{3+}, \text{In}^{3+}$) synthesized by a solid-state reaction at 1100°C .

$2p$ -levels in MO_6 and the conduction band assumed by d -levels in MO_6 when the compound contains octahedral MO_6 .¹⁴ The process for photocatalysis of semiconductors is the direct absorption of photons by the band gap of the materials and generation of electron–hole pairs in the semiconductor particles. The excitation of an electron from the valence band to the conduction band is initiated by light absorption with energy equal to or greater than the band gap of the semiconductor. Upon photon excitation the separated electron and hole can follow along the surface of the solid. If the conduction band potential level of semiconductor is more negative than that of hydrogen evolution, and the valence band potential level is more positive than that of oxygen evolution, decomposition of water can occur even without applying electric power. The potentials of the conduction band of $\text{Bi}_2\text{MnNbO}_7$ ($M = \text{Al}^{3+}, \text{Ga}^{3+}, \text{In}^{3+}$) should be more negative than that of hydrogen evolution and the potentials of the valence band should be more positive than that of oxygen evolution, leading to H_2 and O_2 evolutions from aqueous solutions. The valence band potentials of the photocatalysts should be the same

because $\text{Bi}_2\text{MnNbO}_7$ ($M = \text{Al}^{3+}, \text{Ga}^{3+}, \text{In}^{3+}$) have the same crystal structure. The little difference of band gaps in the photocatalysts might result from that of conduction band. The conduction band of $\text{Bi}_2\text{MnNbO}_7$ ($M = \text{Al}^{3+}, \text{Ga}^{3+}, \text{In}^{3+}$) should be slightly changed toward negative since the band gaps of $\text{Bi}_2\text{MnNbO}_7$ increase with decreasing M^{3+} ionic radii. The surface areas of the photocatalysts are the same as shown in Table 1. It is hard to consider that the differences of the surface areas led to the observed differences of the photocatalytic activity. Thus the difference in the photocatalytic activity of the photocatalysts may be mainly due to the differences of conduction bands. This hypothesis is consistent with Figure 3 where the photocatalytic activity increases with the increasing band gaps (Figure 5).

Xu et al.^{18,19} have studied the electronic conductivity of niobate compounds consisting of chains/layers of NbO_6 octahedron. They found that the $[\text{NbO}_3]_\infty$ chains favor the formation of a narrow conduction band and a possible delocalization of the charge carriers. Conductivity measurements suggest that photogenerated electron–hole pairs in $\text{Bi}_2\text{InNbO}_7$ can move easily in this direction.⁸ The mobility of electron–hole pairs affects the photocatalytic activity, because it affects the probability of electrons and holes reaching reaction sites on the surface of the photocatalysts. This suggests that although the photocatalysts have similar structures, the movement of electrons may be easier in the bond of $M\text{—O—M}$ in $\text{Bi}_2\text{AlNbO}_7$ than in $\text{Bi}_2\text{GaNbO}_7$ and $\text{Bi}_2\text{InNbO}_7$, due to differences in $M\text{—O—M}$ bond angles. Kudo et al.¹⁵ found similar results of the photocatalytic activity in layered perovskite structures $\text{Sr}_2\text{Ta}_2\text{O}_7$ and $\text{Sr}_2\text{Nb}_2\text{O}_7$ consisting of MO_6 ($M = \text{Nb}^{5+}, \text{Ta}^{5+}$) octahedron. They found that the bond angles of $M\text{—O—M}$ in $\text{Sr}_2\text{Ta}_2\text{O}_7$ are close to an ideal perovskite structure, while the $M\text{—O—M}$ bond angles in $\text{Sr}_2\text{Nb}_2\text{O}_7$ are twisted. The photocatalytic activity of $\text{Sr}_2\text{Ta}_2\text{O}_7$ is higher than that of $\text{Sr}_2\text{Nb}_2\text{O}_7$ because the photogenerated electron–hole pairs in $\text{Sr}_2\text{Ta}_2\text{O}_7$ can move more easily than in $\text{Sr}_2\text{Nb}_2\text{O}_7$. The study of the influence of crystal structure on luminescent properties of tantalates and niobates showed that the closer the bond angle of $M\text{—O—M}$ is to the ideal 180° the more the excitation energy is delocalized.^{20–22} This means that the bond angle of $M\text{—O—M}$ is one of the most important factors affecting the photocatalytic and photophysical properties of semiconductors.

It is interesting to note that $\text{Bi}_2\text{MnNbO}_7$ show photoabsorption in the visible light region ($\lambda > 420$ nm), but the photoabsorption is weak. This means that the photocatalysts have the ability to respond to wavelengths in the visible light region. However, these photocatalysts do not work under visible light irradiation ($\lambda > 420$ nm) in our experiment. Alig et al. have

(15) Kudo, A.; Kato, H.; Nakagawa, S. *J. Phys. Chem. B* **2000**, 104, 571.

(16) Alig, R. C.; Bloom, S. W. *Phys. Rev. B* **1980**, 22, 5565.

(17) Linsebigler, A. L.; Lu, G.; Yates, J. T., Jr. *Chem. Rev.* **1995**, 95, 735.

(18) Xu, J.; Greenblatt, M. *J. Solid State Chem.* **1996**, 121, 273.

(19) Xu, J.; Emge, T.; Ramanujachary, K. V.; Hohn, P.; Greenblatt, M. *J. Solid State Chem.* **1996**, 125, 192.

(20) Blasse, G. *J. Solid State Chem.* **1988**, 72, 72.

(21) Blasse, G.; Brixner, L. H. *J. Mater. Res. Bull.* **1989**, 24, 363.

(22) Srivastava, A. M.; Ackerman, J. F. *J. Solid State Chem.* **1997**, 134, 187.

(14) Scaife, D. E. *Sol. Energy* **1980**, 25, 41.

shown that direct absorption of photons by the band gap of oxides can generate electron–hole pairs in the solid.^{16,17} However, the energy of requirement is generally higher than the band gap of the oxides, due to the fact that in the process of splitting water into H₂ and O₂ by photocatalysis at least 4 holes and 2 electrons are necessary on the surface of the photocatalysts. This suggests that much larger energy than the band gap is necessary for splitting water into H₂ and O₂ by photocatalysis. To remove the separated electrons and holes from the photocatalysts to the surface, two ways are possible: One is modification of the surface of the photocatalysts, which may assist modification of the energy levels of the electron and hole. The other is direct increase of the energy of light. BET measurement showed that the surface areas of Bi₂MNbO₇ (M = Al³⁺, Ga³⁺, In³⁺) are 0.51(3), 0.52(1), and 0.51(5) m²/g, respectively. This is about 1% of that of the TiO₂ photocatalyst (53.80(2)) m²/g. On the other hand, the SEM analysis showed that the powder particle size is so large, a maximum size of about 6.0 μm. Since an efficient photocatalytic reaction process occurs on the photocatalyst surface, the smaller surface area of the Bi₂MNbO₇ (M = Al³⁺, Ga³⁺, In³⁺) photocatalysts might lead to the

decrease of effective photocatalytic reaction. The study of the effects of surface area on the photocatalytic reaction and on the range of responding wavelength is in progress.

In summary, the change of M³⁺ ionic radii in Bi₂MNbO₇ (M = Al³⁺, Ga³⁺, In³⁺) pyrochlore could cause the change of carrier concentration and a slight modification of structure. It might cause change of conduction band of the photocatalysts and delocalization/localization of the carriers. The lattice parameters decrease with decreasing M³⁺ ionic radii. However, the activity of the Bi₂MNbO₇ (M = Al³⁺, Ga³⁺, In³⁺) photocatalysts strongly increased with decreasing M³⁺ ionic radii. The study of modification of structure by controlling the ionic radius in photocatalysts for improving the activity will provide useful information on the mechanism of photocatalysts and also on making photocatalysts with high activity.

Acknowledgment. The authors would like to thank Dr. K. Sayama for his valuable discussion and appreciate the contributions of Dr. R. Abe and K. Hara.

CM000687M